Six-rowed spike4 (*Vrs4*) controls spikelet determinacy and row-type in barley

Ravi Koppolu[a,1], Nadia Anwar[b,1], Shun Sakuma[b], Akemi Tagiri[b], Udda Lundqvist[c], Mohammad Pourkheirandish[b], Twan Rutten[d], Christiane Seiler[e], Axel Himmelbach[a], Ruvini Ariyadasa[a], Helmy Mohamad Youssef[a,f], Nils Stein[a], Nese Sreenivasulu[e,g,h], Takao Komatsuda[b], and Thorsten Schnurbusch[a,2]

[a]Department of Genebank, Leibniz-Institute of Plant Genetics and Crop Plant Research (IPK), Gatersleben D06466, Germany; [b]Plant Genome Research Unit, National Institute of Agrobiological Sciences (NIAS), Tsukuba 3058602, Japan; [c]Nordic Genetic Resource Center, Alnarp SE-23053, Sweden; [d]Department of Physiology and Cell Biology, Leibniz-Institute of Plant Genetics and Crop Plant Research (IPK), Gatersleben D06466, Germany; [e]Department of Molecular Genetics, Leibniz-Institute of Plant Genetics and Crop Plant Research (IPK), Gatersleben D06466, Germany; [f]Department of Plant Physiology, Faculty of Agriculture, Cairo University, Giza 12613, Egypt; [g]Research Group Abiotic Stress Genomics, Interdisciplinary Center for Crop Plant Research (IZN), Halle (Saale) D06120, Germany; and [h]Grain Quality and Nutrition Center, International Rice Research Institute (IRRI), Metro Manila 1301, Philippines

Edited by George Coupland, Max Planck Institute for Plant Breeding Research, Cologne, Germany, and approved June 26, 2013 (received for review December 16, 2012)

Inflorescence architecture of barley (*Hordeum vulgare* L.) is common among the Triticeae species, which bear one to three single-flowered spikelets at each rachis internode. Triple spikelet meristem is one of the unique features of barley spikes, in which three spikelets (one central and two lateral spikelets) are produced at each rachis internode. Fertility of the lateral spikelets at triple spikelet meristem gives row-type identity to barley spikes. Six-rowed spikes show fertile lateral spikelets and produce increased grain yield per spike, compared with two-rowed spikes with sterile lateral spikelets. Thus, far, two loci governing the row-type phenotype were isolated in barley that include *Six-rowed spike1* (*Vrs1*) and *Intermedium-C*. In the present study, we isolated *Six-rowed spike4* (*Vrs4*), a barley ortholog of the maize (*Zea mays* L.) inflorescence architecture gene *RAMOSA2* (*RA2*). Eighteen coding mutations in barley *RA2* (*HvRA2*) were specifically associated with lateral spikelet fertility and loss of spikelet determinacy. Expression analyses through mRNA in situ hybridization and microarray showed that *Vrs4* (*HvRA2*) controls the row-type pathway through *Vrs1* (*HvHox1*), a negative regulator of lateral spikelet fertility in barley. Moreover, *Vrs4* may also regulate transcripts of barley *SISTER OF RAMOSA3* (*HvSRA*), a putative trehalose-6-phosphate phosphatase involved in trehalose-6-phosphate homeostasis implicated to control spikelet determinacy. Our expression data illustrated that, although RA2 is conserved among different grass species, its down-stream target genes appear to be modified in barley and possibly other species of tribe Triticeae.

cytokinin | EGG APPARATUS1 | grain number | yield potential

Inflorescence architecture is highly diverse among members of the grass family (Poaceae), in which spikelets represent the fundamental building blocks, comprising one or more florets enclosed by two glumes. Economically important grass species of the tribe Triticeae, such as wheat (*Triticum spp*.), barley, triticale (×*Triticosecale* Wittm. ex A. Camus), and rye (*Secale cereale* L.), typically possess a branchless spike-shaped inflorescence, whereas inflorescences of tropical species, e.g., maize, *Sorghum* spp., and rice (*Oryza sativa* L.), have highly branched tassels or panicles. Inflorescence branching in maize appears to be largely regulated through the *RAMOSA* gene network, which involves the *RAMOSA1* (*RA1*), *RA2*, *RA3*, and *RAMOSA1 ENHANCER LOCUS2* (*REL2*) genes (1). In maize, determinacy of the spikelet pair meristems (SPMs) is mediated through *RA2*, which encodes a lateral organ boundaries (LOB) domain-containing transcriptional regulator that functions upstream of the RA1 and REL2 determinacy-providing complex (2–4). Expression of *RA1* is dependent upon *RA3*, which encodes a phosphatase involved in trehalose metabolism (5). Orthologs of *RA1* and *RA3* are unique to the grass tribe Andropogoneae (paired spikelets arise from SPMs), but close paralogs of *RA3*, with an as of yet unknown function, exist in barley (*HvSRA*) and other grasses (5).

The barley inflorescence is an indeterminate spike that produces three single-flowered spikelets in a distichous manner at each rachis internode that develop into one central and two lateral spikelets (Fig. 1*A*) (6, 7). Based upon lateral spikelet/floret size and fertility barley is classified into two different row-types; i.e., two-rowed and six-rowed barley (8). In two-rowed barley, the central spikelet is fertile and produces grain, and the two lateral spikelets remain sterile (Fig. 1*G*). In six-rowed barley, all three spikelets are fertile and develop into grains (Fig. 1*B*). The six-rowed phenotype is controlled by at least five independent loci that include *Six-rowed spike1* (*vrs1*), *vrs2*, *vrs3*, *vrs4*, and *Intermedium-C* (*Int-c*). *Vrs1* encodes a homeodomain-leucine zipper class I transcription factor that is a negative regulator of lateral spikelet fertility (9). Mutant *vrs1.a* promotes lateral spikelet fertility resulting in a complete six-rowed spike (Fig. 1*B*). Alleles at the locus *int-c*, which is an ortholog of the maize domestication gene *TEOSINTE BRANCHED1* (*HvTB1*) (10), modify lateral spikelet development with respect to allelic constitution at *vrs1* (Fig. 1*F*). Loss-of-function *vrs1.a* is generally accompanied by *Int-c.a* in six-rowed barley and the functional *Vrs1.b* by *int-c.b* in two-rowed barley. The remaining *vrs* loci *vrs2*, *vrs3*, and *vrs4* show varying levels of lateral spikelet fertility with complete lateral spikelet fertility observed in *vrs4* mutants (Fig. 1 *C*–*E*). Apart from lateral spikelet fertility, *vrs4* mutants show indeterminate triple spikelet meristems (TSMs), thereby producing additional spikelets/florets. The apparent indeterminacy of the TSM in *vrs4* mutants suggests that *vrs4* is involved in a genetic pathway that regulates the highly conserved determinate nature of the TSM inherent to *Hordeum* species.

In the present study, we isolated the *vrs4* locus through genetic mapping and extensive mutant analysis. Our findings showed that *Vrs4* underlies *HvRA2*, an ortholog of maize transcription factor *RAMOSA2*, which is important for inflorescence development in grasses. Tissue localization through mRNA in situ hybridization in immature spikes showed that *HvRA2* is expressed very early during inflorescence development and most probably confines barley's TSM meristem to three spikelets. Gene expression analysis in combination with microarray experiments

Author contributions: N. Sreenivasulu, T.K., and T.S. designed research; R.K., N.A., S.S., A.T., U.L., M.P., T.R., C.S., A.H., R.A., and H.M.Y. performed research; N. Stein contributed new reagents/analytic tools; R.K., N.A., S.S., A.T., U.L., M.P., N. Sreenivasulu, T.K., and T.S. analyzed data; and R.K., N.A., S.S., N. Sreenivasulu, T.K., and T.S. wrote the paper.

The authors declare no conflict of interest.

This article is a PNAS Direct Submission.

Freely available online through the PNAS open access option.

Data deposition: The sequences reported in this paper have been deposited in the GenBank database (accession nos.: KC854546–KC854554).

[1]R.K. and N.A. contributed equally to this work.

[2]To whom correspondence should be addressed. E-mail: thor@ipk-gatersleben.de.

This article contains supporting information online at www.pnas.org/lookup/suppl/doi:10.1073/pnas.1221950110/-/DCSupplemental.

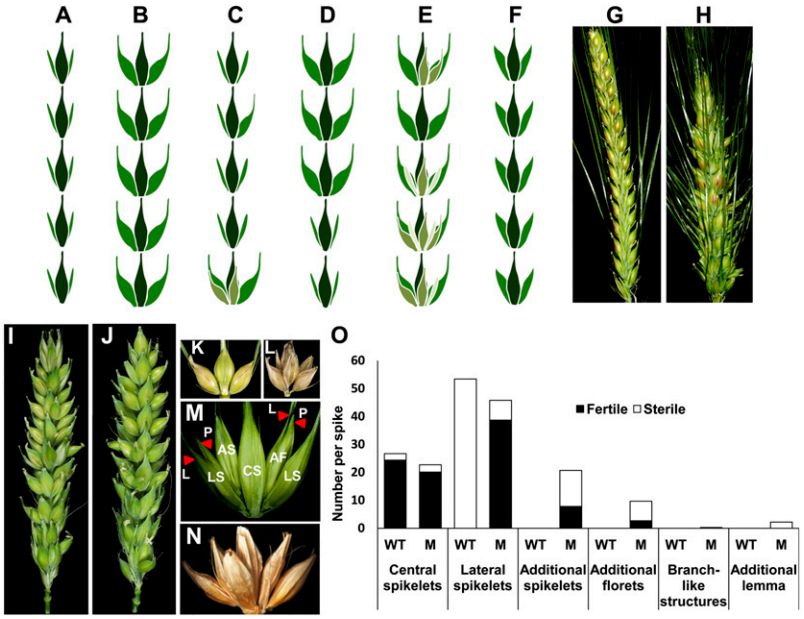

Fig. 1. Spike morphology of different row-type loci and *vrs4* phenotype. (*A*) *Two-rowed spike* (*Vrs1*): fertile central spikelets (CS) and sterile lateral spikelets (LS). (*B*) *Six-rowed spike1* (*vrs1*): completely fertile CS and LS. (*C*) *Six-rowed spike2* (*vrs2*): LS fertility observed at the spike base with occasional additional spikelets [additional spikelet (AS) fertile or sterile, AS in light green color]; along the spike, LS are occasionally enlarged and set seed, (*D*) *Six-rowed spike3* (*vrs3*): spike base appears two-rowed, and the remaining portion appears six-rowed. (*E*) *Six-rowed spike4* (*vrs4*): spike similar to *vrs1*, with frequent awn bearing AS (light green colored). (*F*) *Intermedium-C* (*int-c*): LS are enlarged, set seed, which are usually smaller than in *vrs1*, LS without awns. (*G*) Two-rowed wild-type spike (Piroline). *vrs4* mutant spikes: (*H*) *vrs4.l*, (*I*) BW-NIL(*mul1.a*). (*J*) BW-NIL(*vrs4.k*): six-rowed-like appearance and formation of AS and additional florets (AF). (*K*) Spikelet triplet at one rachis internode. (*L* and *M*) BW-NIL(*vrs4.k*) (*L*) and *vrs4.l* (*M*) showing AS and AF; initial triplet: CS, LS with lemma (L) and palea (P). AF developed on the rachilla of LS. (*N*) Seed formation involving AS and AF. (*O*) Classes of axillary structures produced by *vrs4* mutant *vrs4.l* and wild-type Piroline spikes. Total number of fertile or sterile axillary structures from autumn grown plants is shown. Data were recorded on five plants with on average two spikes per plant. (see SI Dataset S1*A* for SE and significance of *t* test).

demonstrated that *HvRA2* may likely function in two distinct pathways, thereby establishing spike architecture through regulation of TSM determinacy and controlling the *Hordeum*-specific row-type pathway.

Results

***vrs4* Mutants Display Indeterminate TSM and Six-Rowed Phenotype.** Unlike maize or sorghum, in which spikelets develop from SPMs, immature barley spikes develop a TSM that arises from the first axillary meristem right after double ridge stage (first reproductive stage). TSMs are determinate and form three distinct mounds producing three secondary axillary meristems (AMs), one central spikelet meristem (CSM) and two lateral spikelet meristems (LSMs) (Fig. 2*A* and *SI Appendix*, Fig. S1*A*). Each spikelet meristem initially differentiates into a pair of glume primordia (Fig. 2*A*), and then into one floral meristem (FM). Scanning electron microscopy (SEM) analysis of wild type and *vrs4* mutants at double ridge stage revealed no morphological differences, suggesting that there is no change in determinacy of AM that gives rise to triple spikelet primordia (Fig. 2 *A* and *B*). The appearance of two additional mounds on either side of the LSMs was the first visible deviation observed in *vrs4* mutant inflorescences (Fig. 2*B*). The additional spikelets/florets emerging at rachis internodes (*SI Appendix*, Fig. S1 *B* and *C*) were frequently fertile and developed into grains (Fig. 1 *L* and *N*). Additional spikelets had the same orientation (lemma primordia on abaxial side) as normal spikelets (Fig. 1*M* and *SI Appendix*, Fig. S1 *A*, *B*, *D*, and *E*). However, additional florets were oriented opposite to the normal spikelet (lemma primordia on the adaxial side showing the alternate orientation of floret formation on the rachilla) and lacked glumes (Fig. 1*M*). Apart from the additional spikelets/florets (Fig. 1*O* and *SI Appendix*, Fig. S1*G*) we rarely found additional pistils (*SI Appendix*, Fig. S1*I*), suggesting that FM determinacy was also affected in *vrs4* mutants. Loss of determinacy became

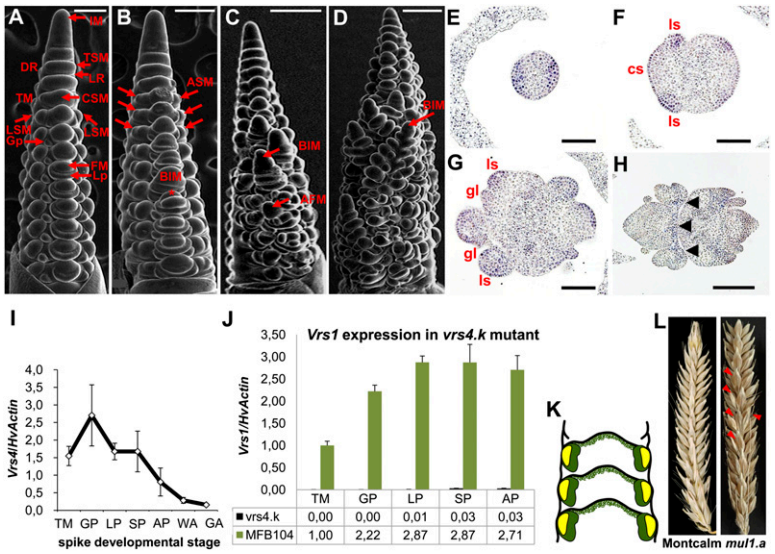

Fig. 2. Scanning electron microscopy and transcript localization of *Vrs4* mRNA in immature barley spikes. (*A*) Wild-type inflorescence at lemma primordium (LP) stage showing inflorescence meristem (IM) forming double ridge (DR), upper ridge containing triple spikelet meristem (TSM), and lower leaf ridge (LR). TSM forms a triple mound (TM), which transitions into one central spikelet meristem (CSM) and two lateral spikelet meristems (LSMs). A pair of glume primordia (GP) and a single floral meristem (FM) are produced by each SM. (*B*) *vrs4* at LP initiating additional spikelet meristems (ASMs) (red arrows). CSMs develop into branch-like inflorescence meristem (BIM). Occasionally, CSMs initiate additional florets on rachilla (asterisk). (*C*) *vrs4* at stamen primordium (SP) stage showing BIM at DR and a developing additional floret meristem (AFM). (*D*) *vrs4* at awn primordium (AP) stage showing BIM at TM. (*E*–*H*) In situ RNA hybridization of *HvRA2* in two-rowed barley cv. Bonus. Transverse sections at DR (*E*), TM (*F*), GP (*G*), and SP (*H*). cs, central spikelet; ls, lateral spikelet; gl, glume. (*I*) Transcript levels of *HvRA2* determined by quantitative RT-PCR in cv. Bonus. Constitutively expressed *HvActin* was used for normalization. X-axis represents spike developmental stages. Mean ± SE of three biological replicates. WA, white anther; GA, green anther. (*J*) *Vrs1* expression in BW-NIL(*vrs4.k*) and wild-type MFB104. Mean ± SE of three biological replicates. Expression values are given at the bottom of the graph. (*K*) *Vrs1* (yellow) and *Vrs4* (green) are expressed in overlapping domains of lateral spikelets. (*L*) Spikes of cv. Montcalm carrying *vrs1.a1* allele and *vrs4* mutant allele *mul1.a*. Additional spikelets in *mul1.a* are indicated by red triangles. (Scale bars: 200 μm in *A* and *B*; 333 μm in *C* and *D*; and 100 μm in *E*–*H*.)

even more apparent when CSMs frequently produced branch-like inflorescence meristems (BIM) with ridges (resembling predouble ridge stage of primary inflorescence) (Fig. 2*C* and *SI Appendix*, Fig. S1*C*), which later differentiated into triple mounds (Fig. 2*D*) and eventually produced a *vrs4*-like inflorescence meristem (*SI Appendix*, Fig. S1*J*). The majority of BIMs aborted as growth continued (*SI Appendix*, Fig. S1 *B* and *C*), and only few meristems at the base developed into additional spikelets. Similar developmental abnormalities were observed in two other *vrs4* Bowman near isogenic alleles BW-NIL(*vrs4.k*) and BW-NIL (*mul1.a*) (*SI Appendix*, Fig. S2 *A*–*E*). SEM analysis revealed that *vrs4* mutants lost determinacy of the TSMs, and subsequently SMs, thus producing supernumerary spikelets and florets. The spring-grown mutant allele *vrs4.1* showed an enhanced *vrs4* phenotype with a significantly higher number of spikelets and branch-like structures than autumn grown plants (*SI Appendix*, Fig. S1 *B* and *C* and SI Dataset S1*A*).

Apart from the indeterminate nature of TSMs, *vrs4* mutants displayed another important feature of complete fertility and development of lateral spikelets resulting in a six-rowed phenotype. The six-rowed phenotype observed in *vrs4* mutants was analogous to that of *vrs1* mutants. In the present study, all *vrs4* mutant alleles, except *int-e.4*, *int-e.20*, and *int-e.72*, showed complete or partial six-rowed phenotype (Fig. 1 *H*–*J* and *SI Appendix*, Fig. S3).

Genetic Mapping and Mutant Analysis Reveals That *Vrs4* Underlies the Barley Ortholog of Maize *RAMOSA2*. We initially mapped *vrs4* to the short arm of chromosome 3H using five F_2 mapping populations comprised of 188–214 gametes (*SI Appendix*, Table S1). Mapped markers were derived from syntenic *Brachypodium* (chromosome 2) and rice (chromosome 1) gene sequences based on the virtual gene order reported in the barley genome zipper (11) (SI Dataset S1*B*). In all five mapping populations tested, the *vrs4* phenotype cosegregated with a cluster of markers (barley orthologs of *Brachypodium*/rice genes) derived from the short arm of 3H (37.17–41.68 cM in genome zipper) (*SI Appendix*, Fig. S4). Flanking markers of the corresponding marker cluster contained 68 predicted *Brachypodium* genes (Bradi2g03717 to Bradi2g04380) (*SI Appendix*, Table S2) within the interval. Using recombinant screens in 2,172 gametes (*vrs4.k* × Golden Promise population), we further refined the interval and mapped *vrs4* to a single BAC contig (1,073 kb) containing at least six predicted genes, including barley *RAMOSA2* (*HvRA2*), *RESURRECTION1* (*RST1*), *TRYPTOPHAN AMINO TRANSFERASE* (TPA), *EMBRYO SAC/BASAL ENDOSPERM TRANSFER LAYER/EMBRYO SURROUNDING REGION* (*EBE*), *STACHYOSE SYNTHASE*, and *RECEPTOR LIKE PROTEIN KINASE* (*INRPK1*) (Fig. 3*D*). Of the six predicted genes, we considered *HvRA2* as an interesting candidate gene for the *Vrs4* locus, because it was identified as being essential for imposing determinacy on SPM identity in maize (3).

Because *vrs4* mutants in general showed loss of determinacy of TSMs, we sequenced *HvRA2* in 20 *vrs4* mutants, and found that 18 showed molecular lesions within the *HvRA2* ORF (Fig. 3*E* and *SI Appendix*, Fig. S5). It had been proposed that the number of meristem primordia giving rise to spikelets is partially unrestricted in *vrs4* mutants resulting in formation of additional spikelets/florets (7). From the mutant analysis, we found that irrespective of the type of lesion in various mutant alleles of *vrs4*, all showed indeterminacy of the TSM to a certain degree (Fig. 1 *H*–*J* and *SI Appendix*, Fig. S3). The molecular nature of the lesions in mutants clearly correlated with the severity of *vrs4* phenotype. Five mutants with the strongest spikelet phenotype had either a premature stop codon [BW-NIL(*vrs4.k*), BW-NIL (*mul1.a*), *vrs4.1* (*syn. Xc 41.5*), *int-e.26* and *int-e.128* (*syn. hex-v.48*)] or a putative gene deletion (MHOR 318 and MHOR 345; Figs. 1 *H*–*J* and 3*E* and *SI Appendix*, Fig. S3). Weaker alleles possessed amino acid substitutions either within the LOB domain [*int-e.23,* BW-NIL(*int-e.58*), *int-e.72*] or in other conserved regions (see below) of the protein (*int-e.65, int-e.66, int-e.87*, *int-e.89, int-e.90*, *int-e.91, int-e.92*, *int-e.101*) (Fig. 3*E* and *SI Appendix*, Fig. S3). The *vrs4* mutants *int-e.4* and *int-e.20* did not show any lesions, suggesting possible transcriptional or post-transcriptional regulation in these alleles (allelism data for *int-e.4* and *int-e.20* with *vrs4* are in *SI Appendix*). The collection of 18 ORF mutants strongly indicated that *HvRA2* underlies the *Vrs4* locus.

***HvRAMOSA2* Encodes a LOB Domain Transcription Factor with Grass-Specific Domains.** HvRA2 is a class I LOB domain protein consisting of a cysteine-rich repeat (CX2CX6CX3C), a highly conserved GAS block, and a Leucine-zipper coiled-coil motif (LX6LX3LX6L) (*SI Appendix*, Fig. S6), signature features conserved in all class I LOB domain proteins (12). Apart from the canonical LOB domain, grasses (monocots) posses a unique C-terminal putative activation domain (44 aa) that is not present in *Arabidopsis* and other eudicots (3) (*SI Appendix*, Fig. S6). Based on sequence alignments generated from orthologous/homologous RA2 proteins from a range of monocot and eudicot species, we identified another conserved grass specific N-terminal region (16 aa) preceding the LOB domain (Fig. 3*E* and *SI Appendix*, Fig. S6). The last four amino acids of the N-terminal domain (PGAG) are strictly conserved across different grass species. Interestingly, seven of the *vrs4* mutants possessed amino acid substitutions in the last four amino acids of the conserved N-terminal region, signifying its putative functional role in grasses. Phylogenetic analysis of RA2 homologs/orthologs in eudicots and monocots grouped them into monocot- and eudicot-specific clades (*SI Appendix*, Fig. S7). Among 23 LOB domain-encoding genes (LBD; 19 class I and four class II) from barley (*SI Appendix*, Table S3), HvRA2 was unique with conserved N- and C-terminal domains and clearly separated from other barley and eudicot LBD family members (*SI Appendix*, Fig. S7 and Table S3).

Resequencing of *HvRA2* in diverse Barley Genotypes Shows Reduced Nucleotide Diversity. In an attempt to identify row-type-specific alleles at *Vrs4* in natural variation, we conducted sequence analysis of the *HvRA2* ORF and parts of the 5′ and 3′ regulatory regions (promoter, UTRs) in a set of 77 diverse two-rowed and six-rowed barley genotypes (SI Dataset S1*C*). Unlike *Vrs1* and *Int-c*, which showed row-type-specific alleles in natural variation (9, 10) *Vrs4* appeared to be conserved across diverse two-rowed and six-rowed germplasm, revealing very low natural nucleotide variation in the coding region (SI Dataset S1*C*). Haplotype analysis using these sequence data resulted in one major and seven minor nucleotide haplotypes (GenBank accession nos. KC854546 to KC854553) without specificity toward a particular geographic region or row-type (*SI Appendix*, Fig. S8 and SI Dataset S1*C*). Among the eight nucleotide haplotypes identified, only one haplotype comprising of the two-rowed genotype, Palmella Blue, coded for an amino acid substitution in an unconserved region of the protein without showing any effect on wild-type phenotype (see SI Dataset S1*C* for protein sequence alignment of nucleotide haplotypes). We found complete conservation in the 3′UTR, suggesting that it may be a target site for *cis*-regulatory elements or involved in mRNA metabolism.

***HvRA2* Is Expressed Early in Spike Development and Functions Upstream of *Vrs1*.** In situ hybridization analyses revealed that the first expression of *HvRA2* was detected during the double ridge stage, when spikelet primordia begin to differentiate (Fig. 2*E*), making *HvRA2* one of the earliest expressed genes during AM differentiation. At triple-mound stage, when spikelet primordia differentiate into three distinct spikelet meristems, *HvRA2* mRNA signals were abundant all over the lateral spikelet primordia with weaker expression in the central spikelet primordia (Fig. 2*F*), indicating a role in providing determinacy and confinement to the TSM. At glume primordium stage, during which floret primordia initiate, *HvRA2* mRNAs were detected in both central and lateral spikelets (Fig. 2*G*). Transcript levels of *HvRA2* in developing spikes at triple mound and glume primordium stages were relatively higher than during later stages (Fig. 2*I*).

Analyzing different six-rowed mutants, Sakuma et al. noticed that *Vrs1* transcripts were particularly down-regulated in the *vrs4*

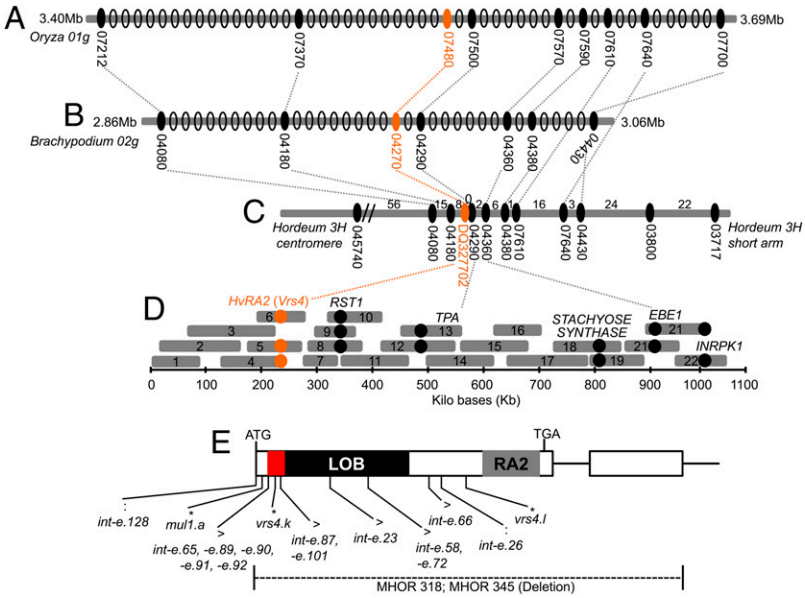

Fig. 3. High-resolution linkage and physical map of *vrs4* and analysis of *vrs4* mutants. (*A*–*C*) Rice (*A*) and *Brachypodium* (*B*) chromosomal regions syntenic with barley chromosome 3H (*C*) in the *vrs4* region. Predicted genes in rice, *Brachypodium* and barley chromosomes are indicated by ovals (Gene names start with *Os01g* (rice) or *Bradi2g* (*Brachypodium*) followed by five digit number). Solid black ovals mark the genes from which markers were derived for mapping in the *vrs4* region. Numbers of recombinants are indicated between mapped markers on the barley chromosome. (*D*) Single BAC contig sequenced in the *vrs4* region (22 overlapping BAC clones covering 1,073 kb) (see *SI Appendix*, Table S5 for corresponding BAC names). Predicted genes identified from the BAC sequences are indicated as circles. (*E*) *HvRA2* gene structure showing a distinct grass-specific domain (red box), and *RA2* as well as the LOB domains. Lesions in 18 ORF-mutant alleles are indicated below the gene structure (see also *SI Appendix*, Fig. S5). :, Nucleotide substitution leading to premature stop codon; *, INDELS leading to frame shift; >, non-synonymous SNP in the coding region.

mutant background (13). We also found that *Vrs1* transcripts in BW-NIL(*vrs4.k*) were significantly lowered at different spike developmental stages (Fig. 2*J*). Unlike *HvRA2* (Fig. 2*E*), *Vrs1* expression in wild-type plants starts at triple-mound stage with no detectable expression during double ridge stage (9). Thus, *HvRA2* expression is temporally ahead of *Vrs1*. Furthermore, *HvRA2* transcripts at triple-mound stage were mainly localized to lateral spikelets (Fig. 2*F*), suggesting an expression domain overlap between VRS1 and HvRA2 proteins (Fig. 2*K*). Consistent with this, most of the *vrs4* mutants showed a complete six-rowed phenotype similar to *vrs1* mutants (Fig. 1 *H*–*J* and *SI Appendix*, Fig. S3), indicating that *Vrs1* transcripts require HvRA2 action. Double mutant analysis supported this view, because *vrs4* allele BW-NIL (*mul1.a*), isolated in a six-rowed background (progenitor: Montcalm, *vrs1.a1*), displayed the six-rowed spike with complete lateral spikelet fertility, as observed in Montcalm, and also indeterminacy of the TSM, diagnostic of *vrs4* mutants (Fig. 2*L*).

Microarray Analysis of *vrs4* Reveals *HvRA2* as an Important Regulator of Inflorescence Development. Because *Vrs4* encodes a LOB domain transcription factor HvRA2, we performed microarray analysis in two *vrs4* deletion mutants, MHOR 318 and MHOR 345, and their respective wild types, Ackermann's Donaria and Heine's Haisa, to identify its potential downstream target genes in barley. From the microarray data, we found compelling evidence for *Vrs4*-mediated regulation of *Vrs1* in both mutants analyzed, with highly significant down-regulation of *Vrs1* in *vrs4* mutants (*SI Appendix*, Fig. S9*A*). Importantly, among other genes significantly down-regulated in both mutants, we identified trehalose-6-phosphate (T6P) synthase and *HvSRA* (a putative T6P phosphatase) (*SI Appendix*, Fig. S9*A*), both involved in trehalose biosynthesis, implying possible regulation of T6P homeostasis by *Vrs4* during inflorescence development and growth (14, 15). From the microarray expression data, we identified other significant differentially regulated genes in both *vrs4* mutants that might likely function in establishing row-type and spikelet determinacy in barley.

The other important differentially regulated gene in both *vrs4* mutants was *EGG APPARATUS1-LIKE* (*EA1-LIKE*). *EA1* encodes a secretary protein that attracts pollen tube growth toward egg apparatus (16). The significant down-regulation of the *EA1-LIKE* gene in wild-type two-rowed inflorescence (*SI Appendix*, Fig. S9*B*) suggests that both *Vrs1* and *EA1-LIKE* may function in a similar pathway. Consistent with this phenomenon, *Vrs1* transcripts show localization to pistils of lateral spikelets in barley (13). Alternatively, elevated expression of *EA1-LIKE* could be due to the proliferating additional spikelets/florets in *vrs4* mutants.

The differentially regulated genes likely involved in enhanced meristematic activity of *vrs4* mutants include *LONELYGUY-LIKE* (*LOG-LIKE*), which encodes cytokinin nucleotide phosphoribohydrolase, a cytokinin biosynthesis enzyme, required to maintain meristem activity (17). Up-regulation of *LOG-LIKE* genes in *vrs4* mutants indicated that higher amounts of *LOG-LIKE* transcripts promoted meristematic activity in *vrs4* mutants (*SI Appendix*, Fig. S9*B*). *LOG1* is required for the accumulation of KNOTTED1-type homeobox (*KNOX*) transcripts in rice (17). Thus, overproduction of cytokinin results in increased steady state levels of *KNOX* gene transcripts (18). Conversely, KNOX proteins were shown to activate cytokinin biosynthesis in the shoot apical meristem of *Arabidopsis* and rice (19, 20). Thus, *KNOX* and cytokinin may act in a positive feedback loop, with *KNOX* genes promoting cytokinin biosynthesis and cytokinins up-regulating *KNOX* biosynthesis. Our data showed up-regulation of *KNAT3* (*KNOX*) in *vrs4* mutants (*SI Appendix*, Fig. S9*B*), suggesting a possible coregulation of LOG-LIKE and KNOX proteins in *vrs4* mutants. The microarray analysis for these differentially regulated genes is supported by quantitative RT-PCR data (*SI Appendix*, Fig. S10).

Independent quantitative RT-PCR analyses of a few important genes (not present on the microarray and identified based on extrapolation of *vrs4* mutant phenotype with known mutant inflorescence architecture genes characterized in rice or maize) revealed differential regulation for cytokinin oxidase/dehydrogenase (*CKX2*), which is involved in cytokinin degradation and meristem size (21). *HvCKX2* transcript levels in BW-NIL(*vrs4.k*) and MHOR 318 were lowered (*SI Appendix*, Fig. S11), consistent with higher meristematic activity in the mutant inflorescence. Transcripts of another gene, *PINFORMED1-LIKE* (*PIN1-LIKE*) (22), were also up-regulated in the *vrs4* mutants, suggesting that altered auxin transport affected lateral organ development in *vrs4* mutants (*SI Appendix*, Fig. S11).

Discussion

The regulation of inflorescence development has been broadly elucidated in plant species, such as *Arabidopsis* and maize (23), with the help of a wealth of mutants that display abnormal inflorescence development. However, in barley, functional knowledge of genes and genetic mechanisms involved in spike development has only started to emerge relatively recently, with the cloning of genes such as *Vrs1* (9) and *Int-c* (10). Mutants of *vrs4*, like other barley row-type mutants, produce a six-rowed phenotype, but the

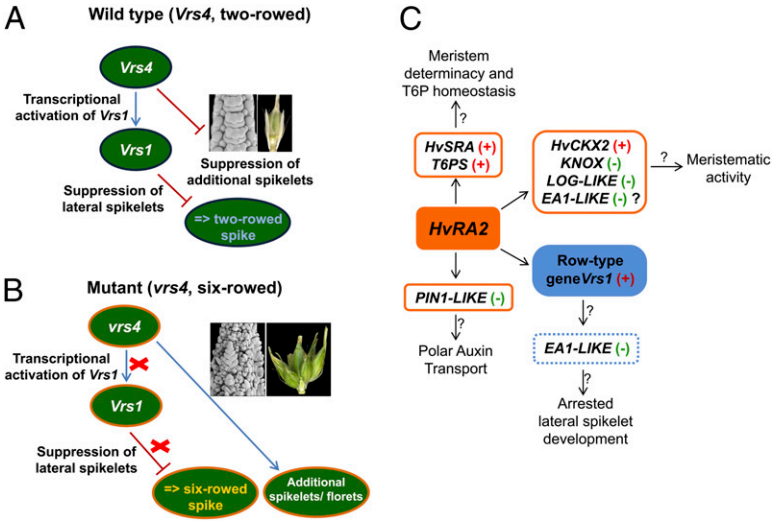

Fig. 4. Models of *Vrs4* interactions showing *HvRA2* putative targets. (*A*) Functional *Vrs4* suppresses additional spikelet formation and activates *Vrs1* transcription. (*B*) Mutant *vrs4* cannot control determinacy of the TSM; thus, additional spikelets are formed. Transcriptional activation of *Vrs1* expression is omitted (red cross) resulting in lateral spikelet fertility. (*C*) *HvRA2* may regulate transcripts of T6P synthase (T6PS) and *HvSRA*, a putative T6P phosphatase, thereby maintaining T6P homeostasis and spikelet determinacy. In *Vrs4*, transcript levels of *PIN1-LIKE* are maintained at constant level but are up-regulated in *vrs4*. In wild-type plants, *HvRA2* functions upstream of *HvHox1*, which in turn may down-regulate transcripts of *EA1-LIKE* resulting in abortion of lateral spikelets, possibly producing a two-rowed spike (hypothetical). However, up-regulation of *EA1-LIKE* in *vrs4* mutants may likely be due to enhanced meristematic activity related to the six-rowed spike phenotype and additional spikelets/florets. Transcript levels of genes involved in meristematic activity [e.g., cytokinin oxidase (*CKX2*), *LONELY GUY-LIKE*, and *KNOX* genes] are also regulated by *HvRA2*.

most interesting phenotype is the indeterminate TSM, resulting in the formation of additional spikelets/florets that frequently develop into grains. Thus, actions of *vrs4*, possibly along with other as of yet unknown genes, may help elucidating how to increase yield potential in barley and other Triticeae species.

Our resequencing data showed very limited natural variation in *HvRA2* across diverse barley germplasm with complete conservation in the 3′UTR. A low level of polymorphisms in the 3′ regulatory region was also observed in maize domestication loci *RA1* (24) and *GRASSY TILLERS1* (25). We hypothesize that naturally occurred variations at this locus might have undergone purifying selection in two- and six-rowed barleys, as severe mutations would disrupt determinacy of the TSM, leading to disordered spike formation. However, weaker natural mutant alleles of *vrs4* might still be hidden among *intermedium* barleys, which represent a large and diverse phenotypic row-type class within cultivated barley.

Another important finding from the present study is the transcriptional regulation of *Vrs1* by HvRA2. Our microarray analysis confirmed that *Vrs1* is significantly down-regulated in *vrs4* mutants. The *HvRA2* mRNA in situ hybridization results showed that *HvRA2* and *Vrs1* are expressed in highly overlapping domains of lateral spikelets, suggesting a putative interaction. Circumstantial evidence supporting this view came from the LOB domain consensus DNA recognition motif 5′-CCGGCG-3′ (26) present in the *Vrs1* promoter region close to the transcriptional start site (−60 to −65 bp) and also in the 5′UTR. Previous in vitro protein binding assays showed strong binding affinity of LOB domain proteins to this consensus motif (26). However, the physical interaction between HvRA2 and *Vrs1 cis* elements needs to be established. Clearly, reduction of *Vrs1* transcripts in *vrs4* mutants indicated that HvRA2 directly or indirectly controls *Vrs1* transcripts, and thus the row-type pathway (Fig. 4 *A* and *B*).

In maize, inflorescence morphology is largely governed by the *RAMOSA* pathway under the coordinated regulation of *RA1*, *RA2*, and *RA3*. Maize *RA3* shows a highly localized expression pattern at the base of inflorescence branches and encodes a functional T6P phosphatase, suggesting a role for trehalose signaling in meristem determinacy (5). A clear ortholog of *RA3* is not present in barley. However, a homolog of *RA3*, termed *SISTER OF RAMOSA3* (*SRA*), has been identified in barley (*HvSRA*) and related grasses (5). The rice homolog of *RA3* (*OsSRA*) also showed highly localized expression pattern at the base of inflorescence branches (5), suggesting a role in inflorescence patterning. In maize, *RA1* transcripts are under the control of *RA2* and *RA3*, whereby RA2 controls the fate of SPMs through the RA1–REL2 determinacy complex (4). The SPM is specific to the tribe Andropogoneae, as is RA1 (1, 2). Thus, HvRA2 seemed to have maintained a conserved function (control over meristem determinacy), but diversified the downstream targets for executing this function in barley (as the ortholog/homolog of *RA1* is missing in barley). In the large barley mutant collection, several spike mutants for the multifloret or branched spike, such as *extra floret* (*flo*)-*a*, *flo-b*, *flo-c*, *compositum1* (*com1*), *com2*, and *multiflorus2* (*mul2*), were reported, but the underlying genes for these mutants have still not been identified. These loci could be potential candidate targets of *Vrs4* for conferring spikelet determinacy. Although *RA2* and *RA3* act independently in maize, we found that *HvRA2* may regulate transcripts of *HvSRA* and T6P synthase, which in turn may regulate specific growth responses through synthesis of T6P (Fig. 4*C*) (27). Moreover, HvRA2 coopted a genus-specific function for the row-type pathway through regulation of *Vrs1* (control over lateral spikelet fertility), thereby clearly indicating different gene sets and networks for inflorescence development compared with maize (Fig. 4*C*). In addition, we showed transcript differences for *HvCKX2* and auxin transporters in *vrs4* mutants, further suggesting a role in inflorescence growth and development (Fig. 4*C*).

Taken together, our results suggest that *Vrs4* is a central player in establishing inflorescence architecture of barley spikes, as well as in determining yield potential and grain number. Thus, a better understanding of the underlying gene regulatory networks during spike formation may help to improve future grain yields of small-grain cereals.

Materials and Methods

Plant Material. Allelic *vrs4* mutants (*SI Appendix*, Table S4) were obtained from the Nordic Genetic Resource Center, the National Small Grains Collection (US Department of Agriculture), and the IPK gene bank. Seventy-seven diverse barley accessions were obtained from IPK gene bank for haplotype analysis. The mutant alleles *vrs4.l* (*syn. Xc 41.5*), its two-rowed progenitor Piroline, and Bowman isolines BW-NIL(*vrs4.k*) and BW-NIL(*mul.1a*) were used for phenotypic descriptions and SEM analysis. Plant material used for generating the mapping populations is discussed in *SI Appendix*.

***Vrs4* Phenotype Characterization.** *vrs4.l* was selected as a reference for comparing inflorescence development with the wild-type Piroline. Piroline and *vrs4.l* were grown in fields in Tsukuba, Japan, during the autumn (October 2011 to June 2012) and spring (March 2012 to June 2012) seasons. For the analysis shown in Fig. 1*O* and SI Dataset S1*A*, data were recorded in five plants (two spikes per plant) from each of the genotypes. Probability values were determined using *t* test. The number of rachis internodes and number of seeds produced by mutant and wild type were counted. A spikelet triplet consisting of three spikelets was considered a basic set of axillary structures and the remaining axillary structures were considered additional axillary structures. Each triplet or multispikelet was divided into one central and two lateral units, and the number of additional spikelets/florets was counted in each unit. An additional axillary structure was counted as a supernumerary floret when the rachilla of the first axillary structure was not visible. The total number of branch-like structures and additional lemma-like structures

produced by a spike were counted. Fertility of axillary structure was scored by counting the number of seeds produced by each type of axillary structure.

Marker Development. For initial mapping, BOPA SNP markers (28) or SSR and EST based markers (SI Dataset S1*B*) were selected from the high-density transcript map of barley chromosome 3H (29). For further marker development in the defined *vrs4* interval, we relied on the barley genome zipper (11). Gene sequences from the syntenic interval in rice or *Brachypodium* were extracted from respective genome browser servers (http://rice.plantbiology.msu.edu/cgi-bin/gbrowse/rice/ and http://jbrowse.brachypodium.org/JBrowse.html). The obtained gene sequences were BLASTed against the IPK Barley BLAST server (http://webblast.ipk-gatersleben.de/barley/viroblast.php) to obtain barley sequences. SNP polymorphisms identified from the primers designed were converted to restriction enzyme based CAPS (30) (http://tools.neb.com/NEBcutter2/) or dCAPS (31) markers (http://helix.wustl.edu/dcaps/).

Quantitative RT-PCR. Total RNA was extracted from immature spike tissues (double ridge, triple mound, glume primordium, lemma primordium, stamen primordium, and awn primordium stages) using the PureLink RNA Mini kit (Invitrogen). RNase-free DNase (Invitrogen) was used to remove genomic DNA contamination. The RNA integrity and quantities were measured using the Agilent Bioanalyzer and NanoDrop (Peq Lab), respectively. Reverse transcription and cDNA synthesis were carried out with 1 μg of RNA using the QuantiTect Reverse Transcription kit (Qiagen). Real-time PCR was performed using the QuantiTect SYBR Green PCR kit (Qiagen) and the ABI Prism 7900HT sequence detection system (Applied Biosystems). RT-PCR results were analyzed using SDS2.2 software (Applied Biosystems). Quantitative RT-PCR primer sequences are listed in SI Dataset S1*B*.

mRNA in Situ Hybridization. The *Vrs4* gene segment comprising parts of the first and second exons (395 bp) was amplified from cDNA isolated from cv. Bonus immature spikes using specific primers (SI Dataset S1*B*). The PCR product was cloned into the pBluescript II KS (+) vector (Stratagene). Clones linearized by EcoRI or NotI were used as templates to generate antisense (EcoRI) and sense (NotI) probes using T3 or T7 RNA polymerase. In situ hybridization was conducted as described (9).

BAC Sequencing, Assembly, and Annotation. A single BAC contig spanning 1,073 kb of the minimum tiling path of barley chromosome 3H was shotgun sequenced using 454 technology (*SI Appendix*, Table S5) (32) and assembled as described (33). ORFs from the BAC sequences were predicted using the Genescan web server (34). The predicted genes were annotated using the BLASTX function of the National Center for Biotechnology Information (NCBI).

Phylogenetic Analysis. Barley LBD genes were extracted from the IPK barley BLAST server using *HvRA2* as a query sequence. HvRA2 protein was used as NCBI BLASTp query to retrieve RA2 and RA2-LIKE proteins (E-value cutoff 10^{-30}) from monocots and eudicots, respectively (*SI Appendix*, Table S6). For phylogenetic analysis, the protein sequences were initially aligned using the MUSCLE algorithm implemented in MEGA 5.1 (35). A maximum likelihood (ML) phylogenetic tree was constructed using the ML heuristic method Nearest Neighbor Interchange (NNI) implemented in MEGA 5.1. The bootstrap consensus tree inferred from 1,000 replicates is taken to represent the evolutionary history of the sequences analyzed. Branches corresponding to partitions reproduced in less than 50% bootstrap replicates are collapsed.

Scanning Electron Microscopy. Immature spike tissues at five stages (triple mound, glume, lemma, stamen, and awn primordium) from field-grown as well as greenhouse-grown plants were used for scanning electron microscopy (SEM). SEM was conducted as described (36).

ACKNOWLEDGMENTS. We thank Dr. S. R. Palakolanu (International Crops Research Institute for the Semi-Arid Tropics) for help with phylogenetic analysis; Dr. B. Kilian (IPK Gatersleben) for providing germplasm for haplotype analysis; H. Bockelman (US Department of Agriculture–Agricultural Research Service) and IPK gene bank for providing initial mutant germplasm; I. Walde for help with the VeraCode experiment; P. Gawroński for helpful discussions; and H. Ernst, H. Koyama, S. König, K. Lipfert, M. Püffeld, M. Pürschel, C. Trautewig, and C. Weißleder for excellent technical support. This work was supported by grants from the Ministry of Education (IZN), Saxony-Anhalt (to N. Sreenivasulu), the Ministry of Agriculture, Forestry, and Fisheries of Japan (Genomics for Agricultural Innovation Grant TRG1004; to T.K.), the Deutsche Forschungsgemeinschaft (DFG Grant SCHN 768/2-1; to T.S.), and the BMBF (German Federal Ministry of Education and Research, GABI-FUTURE Start_Young Investigator Program Grant 0315071; to T.S.).

1. Kellogg EA (2007) Floral displays: Genetic control of grass inflorescences. *Curr Opin Plant Biol* 10(1):26–31.
2. Vollbrecht E, Springer PS, Goh L, Buckler ES, Martienssen R (2005) Architecture of floral branch systems in maize and related grasses. *Nature* 436(7054):1119–1126.
3. Bortiri E, et al. (2006) *ramosa2* encodes a LATERAL ORGAN BOUNDARY domain protein that determines the fate of stem cells in branch meristems of maize. *Plant Cell* 18(3):574–585.
4. Gallavotti A, et al. (2010) The control of axillary meristem fate in the maize *ramosa* pathway. *Development* 137(17):2849–2856.
5. Satoh-Nagasawa N, Nagasawa N, Malcomber S, Sakai H, Jackson D (2006) A trehalose metabolic enzyme controls inflorescence architecture in maize. *Nature* 441(7090): 227–230.
6. Sreenivasulu N, Schnurbusch T (2012) A genetic playground for enhancing grain number in cereals. *Trends Plant Sci* 17(2):91–101.
7. Forster BP, et al. (2007) The barley phytomer. *Ann Bot (Lond)* 100(4):725–733.
8. Mansfeld R (1950) Das morphologische System der Saatgerste, *Hordeum vulgare* L.s.l. *Der Züchter* 20:8–24.
9. Komatsuda T, et al. (2007) Six-rowed barley originated from a mutation in a homeodomain-leucine zipper I-class homeobox gene. *Proc Natl Acad Sci USA* 104(4):1424–1429.
10. Ramsay L, et al. (2011) *INTERMEDIUM-C*, a modifier of lateral spikelet fertility in barley, is an ortholog of the maize domestication gene *TEOSINTE BRANCHED 1*. *Nat Genet* 43(2):169–172.
11. Mayer KF, et al. (2011) Unlocking the barley genome by chromosomal and comparative genomics. *Plant Cell* 23(4):1249–1263.
12. Shuai B, Reynaga-Peña CG, Springer PS (2002) The *lateral organ boundaries* gene defines a novel, plant-specific gene family. *Plant Physiol* 129(2):747–761.
13. Sakuma S, et al. (2013) Divergence of expression pattern contributed to neofunctionalization of duplicated HD-Zip I transcription factor in barley. *New Phytol* 197(3):939–948.
14. Schluepmann H, Berke L, Sanchez-Perez GF (2012) Metabolism control over growth: A case for trehalose-6-phosphate in plants. *J Exp Bot* 63(9):3379–3390.
15. Eveland AL, Jackson DP (2012) Sugars, signalling, and plant development. *J Exp Bot* 63(9):3367–3377.
16. Márton ML, Cordts S, Broadhvest J, Dresselhaus T (2005) Micropylar pollen tube guidance by egg apparatus 1 of maize. *Science* 307(5709):573–576.
17. Kurakawa T, et al. (2007) Direct control of shoot meristem activity by a cytokinin-activating enzyme. *Nature* 445(7128):652–655.
18. Rupp H-M, Frank M, Werner T, Strnad M, Schmülling T (1999) Increased steady state mRNA levels of the *STM* and *KNAT1* homeobox genes in cytokinin overproducing *Arabidopsis thaliana* indicate a role for cytokinins in the shoot apical meristem. *Plant J* 18(5):557–563.
19. Yanai O, et al. (2005) Arabidopsis KNOXI proteins activate cytokinin biosynthesis. *Curr Biol* 15(17):1566–1571.
20. Sakamoto T, et al. (2006) Ectopic expression of KNOTTED1-like homeobox protein induces expression of cytokinin biosynthesis genes in rice. *Plant Physiol* 142(1):54–62.
21. Ashikari M, et al. (2005) Cytokinin oxidase regulates rice grain production. *Science* 309(5735):741–745.
22. Gälweiler L, et al. (1998) Regulation of polar auxin transport by *AtPIN1* in Arabidopsis vascular tissue. *Science* 282(5397):2226–2230.
23. Malcomber ST, Preston JC, Reinheimer R, Kossuth J, Kellogg EA (2006) Developmental gene evolution and the origin of grass inflorescence diversity. *Adv Bot Res* 44:425–481.
24. Sigmon B, Vollbrecht E (2010) Evidence of selection at the *ramosa1* locus during maize domestication. *Mol Ecol* 19(7):1296–1311.
25. Whipple CJ, et al. (2011) *grassy tillers1* promotes apical dominance in maize and responds to shade signals in the grasses. *Proc Natl Acad Sci USA* 108(33):E506–E512.
26. Husbands A, Bell EM, Shuai B, Smith HM, Springer PS (2007) LATERAL ORGAN BOUNDARIES defines a new family of DNA-binding transcription factors and can interact with specific bHLH proteins. *Nucleic Acids Res* 35(19):6663–6671.
27. Eveland AL, et al. (2010) Digital gene expression signatures for maize development. *Plant Physiol* 154(3):1024–1039.
28. Close TJ, et al. (2009) Development and implementation of high-throughput SNP genotyping in barley. *BMC Genomics* 10:582.
29. Sato K, Nankaku N, Takeda K (2009) A high-density transcript linkage map of barley derived from a single population. *Heredity (Edinb)* 103(2):110–117.
30. Vincze T, Posfai J, Roberts RJ (2003) NEBcutter: A program to cleave DNA with restriction enzymes. *Nucleic Acids Res* 31(13):3688–3691.
31. Neff MM, Turk E, Kalishman M (2002) Web-based primer design for single nucleotide polymorphism analysis. *Trends Genet* 18(12):613–615.
32. Meyer M, Stenzel U, Hofreiter M (2008) Parallel tagged sequencing on the 454 platform. *Nat Protoc* 3(2):267–278.
33. Steuernagel B, et al. (2009) *De novo* 454 sequencing of barcoded BAC pools for comprehensive gene survey and genome analysis in the complex genome of barley. *BMC Genomics* 10:547.
34. Burge C, Karlin S (1997) Prediction of complete gene structures in human genomic DNA. *J Mol Biol* 268(1):78–94.
35. Tamura K, et al. (2011) MEGA5: Molecular evolutionary genetics analysis using maximum likelihood, evolutionary distance, and maximum parsimony methods. *Mol Biol Evol* 28(10):2731–2739.
36. Lolas IB, et al. (2010) The transcript elongation factor FACT affects Arabidopsis vegetative and reproductive development and genetically interacts with HUB1/2. *Plant J* 61(4):686–697.